# Structural basis for energy transfer and electron transport in the photosystem I-ferredoxin-$NADP^+$ reductase supercomplex from *Nannochloropsis oceanica*

Yue Qiu[1], Hui Shang[1], Ruiqi Shao[1], Qingyang Li[1], Jiaqi Meng[1], Xiaodong Su[2], Shumeng Zhang[2], Mei Li[2,*] and Xiaowei Pan[1,*]

1. Beijing Key Laboratory of Plant Gene Resources and Biotechnology for Carbon Reduction and Environmental Improvement, College of Life Science, Capital Normal University, Beijing 100048, China.
2. State Key Laboratory of Biomacromolecules, Institute of Biophysics, Chinese Academy of Sciences, Beijing 100101, China.

* Correspondences: Mei Li (meili@ibp.ac.cn), Xiaowei Pan (panxw@cnu.edu.cn)

## Supplementary Information

This file contains:
Supplementary Figures 1-10
Supplementary Tables 1-5

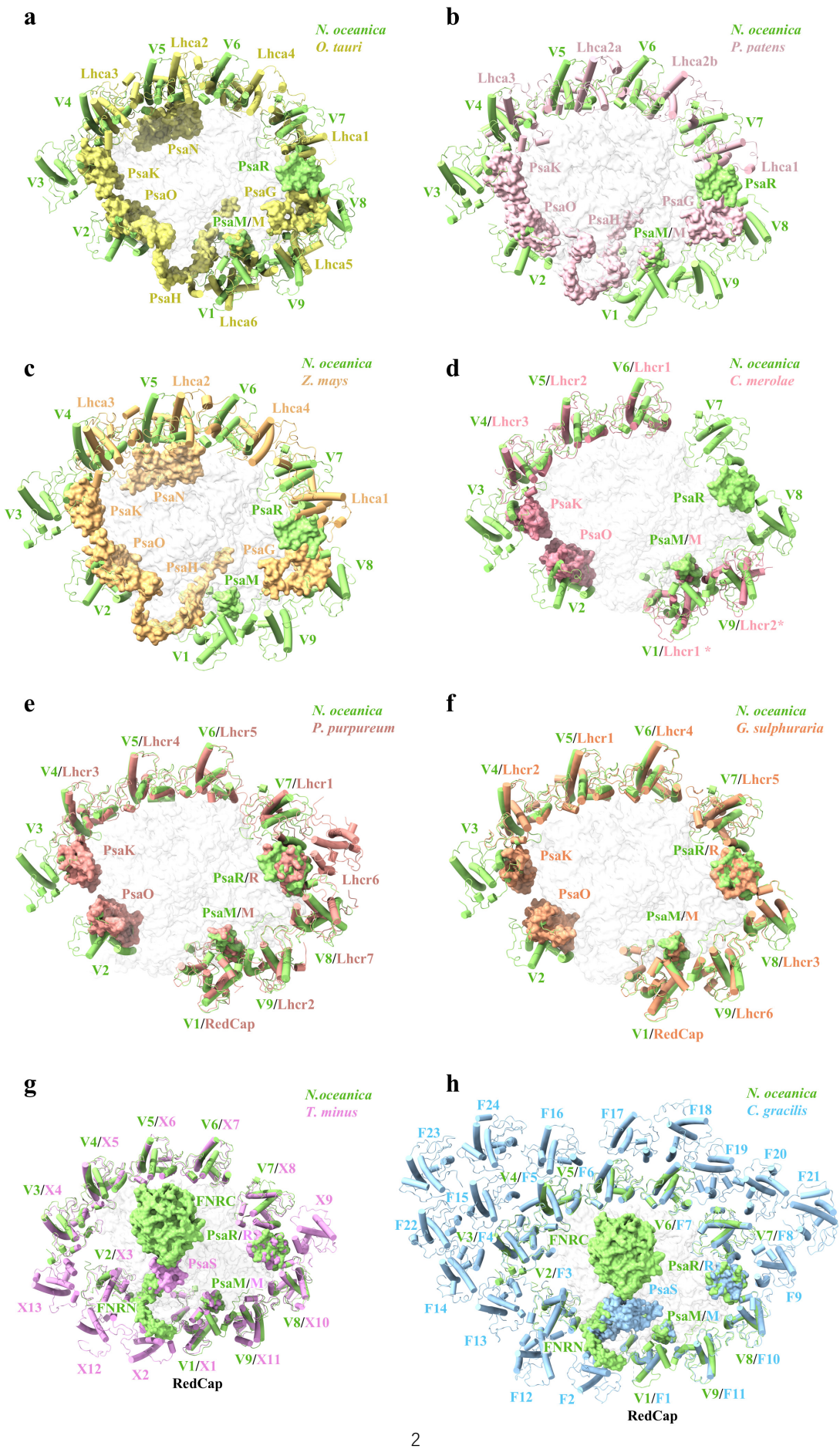
a
N. oceanica
O. tauri
V5
Lhca2
V6
Lhca4
Lhca3
V4
V7
Lhca1
PsaN
PsaR
PsaK
V3
PsaO
PsaG
V8
PsaM/M
V2
Lhca5
PsaH
V1
V9
Lhca6
b
N. oceanica
P. patens
V5
Lhca2a
V6
Lhca2b
Lhca3
V4
V7
PsaK
Lhca1
PsaR
V3
PsaO
PsaG
PsaH
PsaM/M
V8
V2
V9
V1
c
N. oceanica
Z. mays
V5
Lhca2
V6
Lhca3
V4
Lhca4
V7
PsaN
Lhca1
V3
PsaK
PsaR
PsaO
PsaG
PsaH
V8
PsaM
V2
V9
V1
d
N. oceanica
C. merolae
V6/Lhcr1
V5/Lhcr2
V4/Lhcr3
V7
V3
PsaK
PsaR
V8
PsaO
PsaM/M
V2
V9/Lhcr2*
V1/Lhcr1 *
e
N. oceanica
P. purpureum
V6/Lhcr5
V5/Lhcr4
V4/Lhcr3
V7/Lhcr1
V3
PsaK
PsaR/R
Lhcr6
PsaO
PsaM/M
V8/Lhcr7
V2
V9/Lhcr2
V1/RedCap
f
N. oceanica
G. sulphuraria
V6/Lhcr4
V5/Lhcr1
V4/Lhcr2
V7/Lhcr5
V3
PsaK
PsaR/R
PsaO
PsaM/M
V8/Lhcr3
V2
V9/Lhcr6
V1/RedCap
g
N.oceanica
T. minus
V5/X6
V6/X7
V4/X5
V7/X8
V3/X4
FNRC
X9
PsaR/R
V2/X3
PsaS
PsaM/M
X13
FNRN
V8/X10
V9/X11
X12
X2
V1/X1
RedCap
h
N. oceanica
C. gracilis
F24
F16
F17
F18
F23
F19
F20
V4/F5
V5/F6
F21
F15
F22
V6/F7
V3/F4
FNRC
V7/F8
PsaR/R
V2/F3
PsaS
F9
F14
PsaM/M
F13
FNRN
V8/F10
F12
F2
V1/F1
V9/F11
RedCap

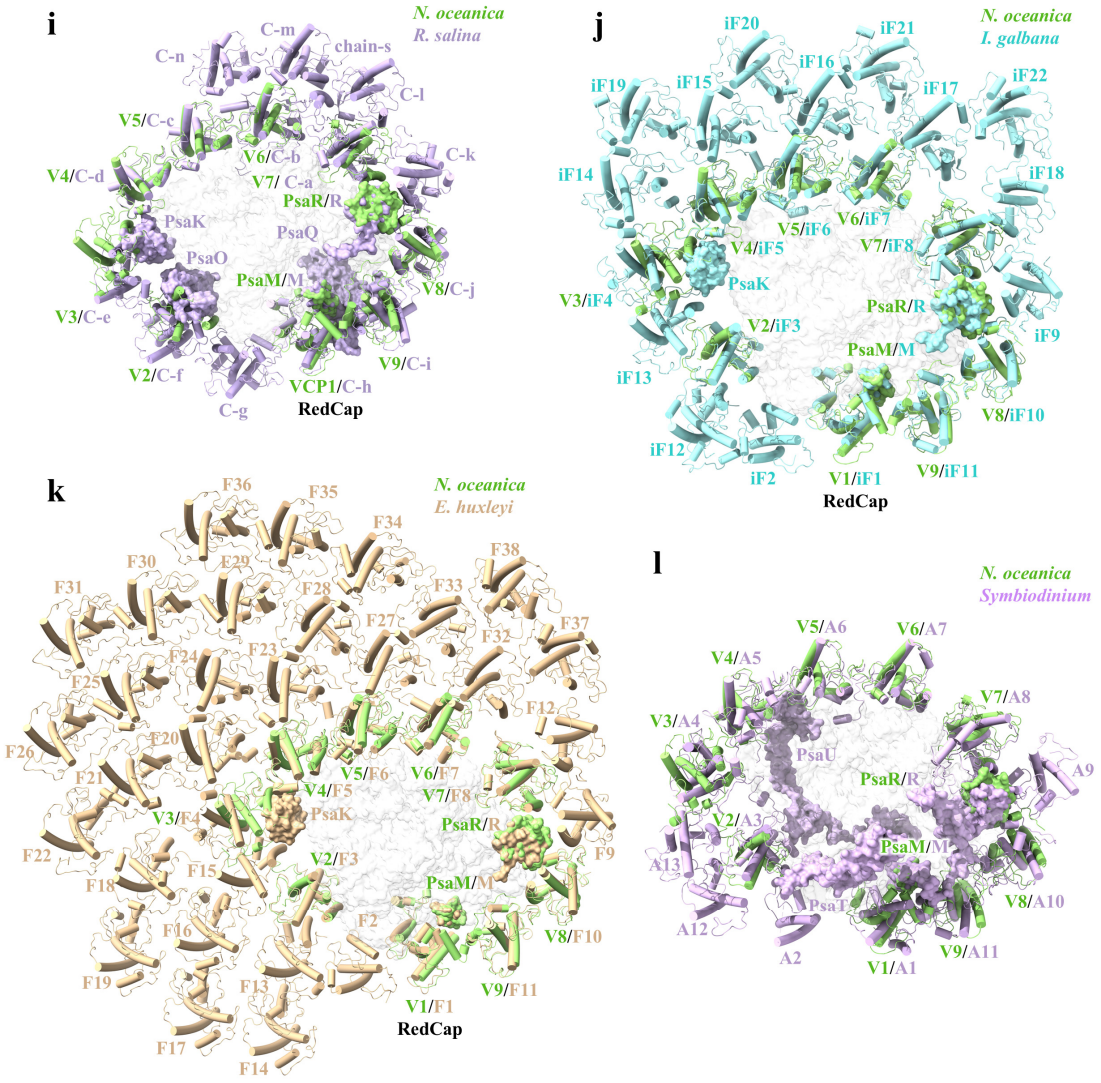


**Supplementary Fig. 1 | Structural comparison of the NoPSI-VCP-FNR supercomplex with PSI-LHCI from representative species.**

**a-l,** Structural comparison of the NoPSI-VCP-FNR supercomplex with PSI-LHCI structures from green algae *Ostreococcus tauri* (*O. tauri*, **a**, 7YCA); moss *Physcomitrium patens* (*P. patens*, **b**, 7KSQ); vascular plant *Zea mays* (*Z. mays*, **c**, 5ZJI); red algae *Cyanidioschyzon merolae* (*C. merolae*, **d**, 5ZGB), *Porphyridium purpureum* (*P. purpureum*, **e**, 7Y5E) and *Galdieria sulphuraria* (*G. sulphuraria*, **f**, 9KC5); xanthophyte *Tribonema minus* (*T. minus*, **g**, 9M4F); diatom *Chaetoceros gracilis* (*C. gracilis*, **h**, 6LY5); cryptophyte *Rhodomonas salina* (*R. salina*, **i**, 8WM6); haptophyte *Isochrysis galbana* (*I. galbana*, **j**, 8Z11); coccolithophore *Emiliania huxleyi* (*E. huxleyi*, **k**, 9JJ8); and dinoflagellate *Symbiodinium* sp. (*Symbiodinium*, **l**, 8JJR). The conserved PSI core subunits are shown in white surface, and species-specific core subunits are colored. For clarity, FNR is displayed only in **g** and **h**. Light-harvesting complexes (LHCIs) are shown in cartoon representation. Labels V, X, F, C, iF, and A denote VCP, XLH, FCPI, CAC, iFCPI, and AcpPCI, respectively.

**a**

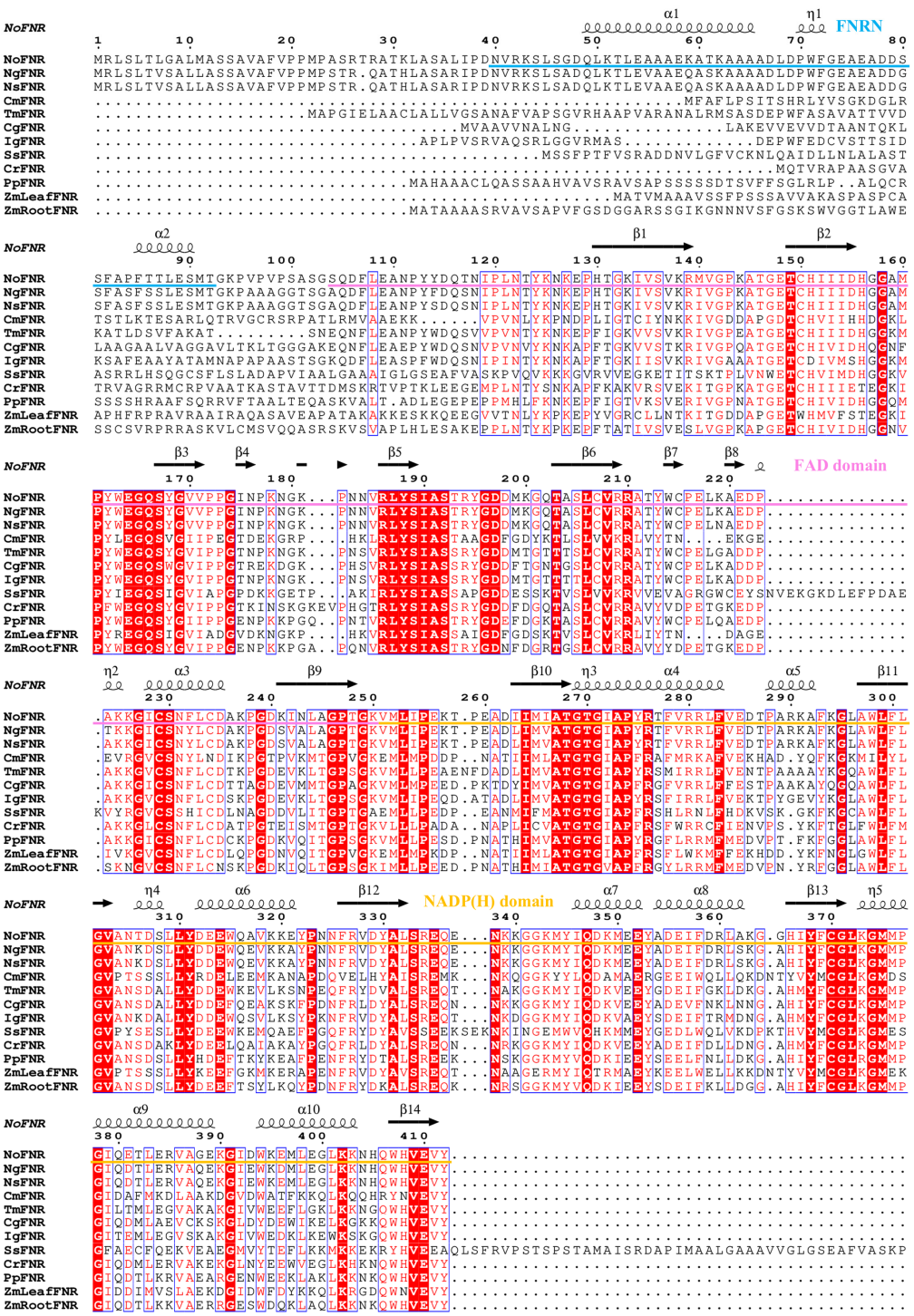
NoFNR
NgFNR
NsFNR
CmFNR
TmFNR
CgFNR
IgFNR
SsFNR
CrFNR
PpFNR
ZmLeafFNR
ZmRootFNR
FNRN
FAD domain
NADP(H) domain

**b**

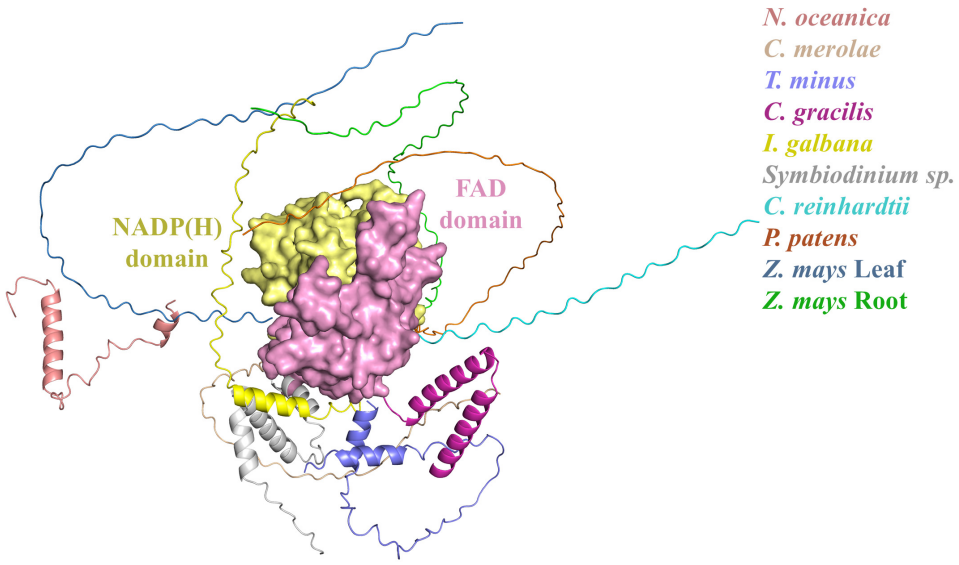


**Supplementary Fig. 2 | Sequence and structural alignment of NoFNR with representative eukaryotic photosynthetic organisms.**

**a**, Sequence alignment of FNR from *N. oceanica* (No) with representative eukaryotic photosynthetic organisms, including *Nannochloropsis gaditana* (Ng), *Nannochloropsis salina* (Ns), red alga *C. merolae* (Cm), xanthophyte *T. minus* (Tm), diatom *C. gracilis* (Cg), haptophyte *I. galbana* (Ig), dinoflagellate *Symbiodinium* sp. (Ss), green alga *C. reinhardtii* (Cr), moss *P. patens* (Pp), and vascular plant *Z. mays* leaf (ZmLeaf) and root (ZmRoot). Fully conserved residues are highlighted in red, and similar amino acids are boxed in blue. The N-terminal, FAD-binding, and NADP(H)-binding domains of NoFNR are indicated by blue, pink, and yellow lines, respectively. **b**, Structural comparison of NoFNR with AlphaFold-predicted models of FNR from representative eukaryotic photosynthetic organisms. The FAD-binding and NADP(H)-binding domains of FNR are depicted as pink and yellow surfaces, respectively, with the N-terminal regions of each FNR shown as cartoons.

**a**

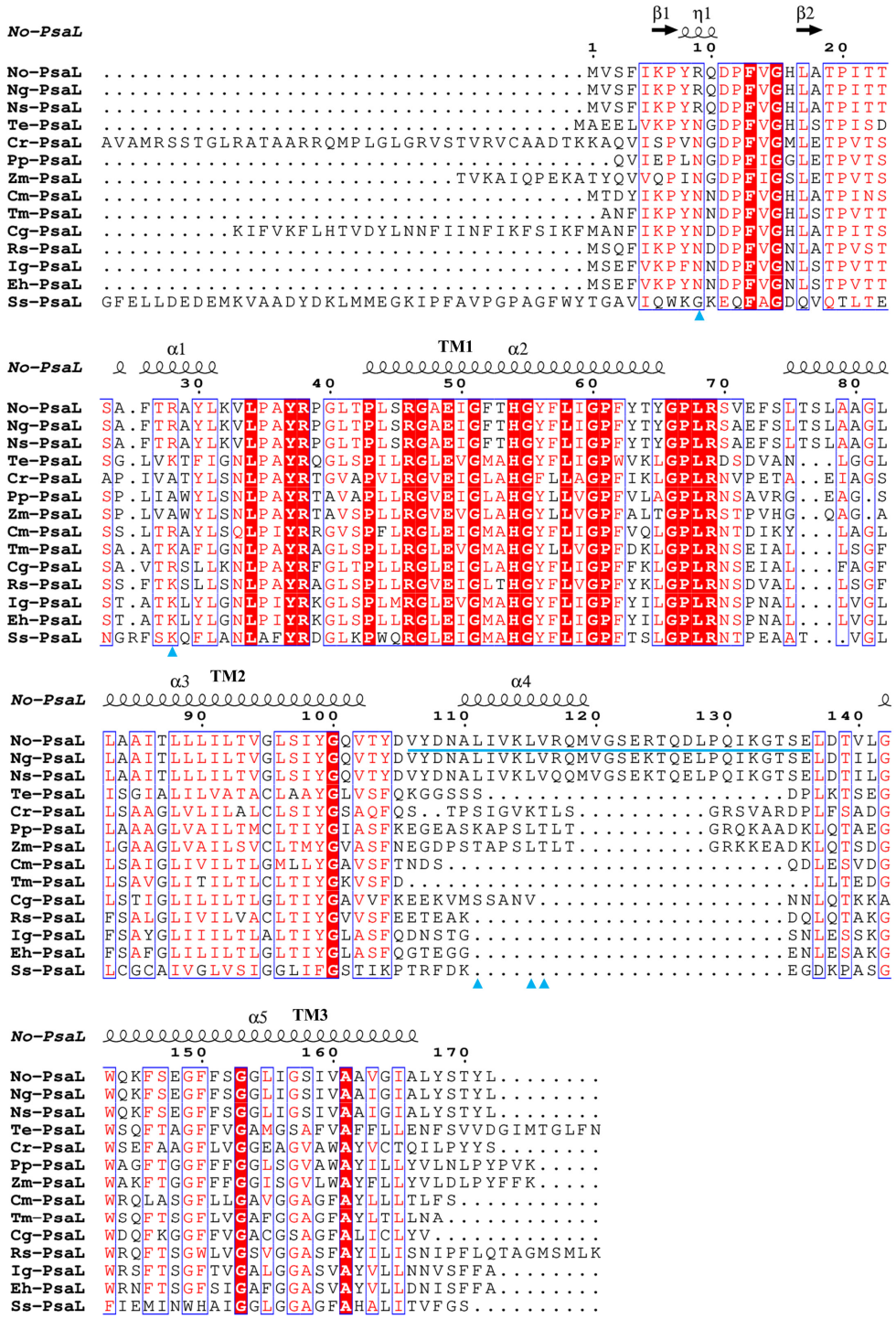
No-PsaL
β1 η1 β2
No-PsaL MVSFIKPYRQDPFVGHLATPITT
Ng-PsaL MVSFIKPYRQDPFVGHLATPITT
Ns-PsaL MVSFIKPYRQDPFVGHLATPITT
Te-PsaL MAEELVKPYNGDPFVGHLSTPISD
Cr-PsaL AVAMRSSTGLRATAARRQMPLGLGRVSTVRVCAADTKKAQVISPVNGDPFVGMLETPVTS
Pp-PsaL QVIEPLNGDPFIGGLETPVTS
Zm-PsaL TVKAIQPEKATYQVVQPINGDPFIGSLETPVTS
Cm-PsaL MTDYIKPYNNDPFVGHLATPINS
Tm-PsaL ANFIKPYNNDPFVGHLSTPVTT
Cg-PsaL KIFVKFLHTVDYLNNFIINFIKFSIKFMANFIKPYNDDPFVGHLATPITS
Rs-PsaL MSQFIKPYNDDPFVGNLATPVST
Ig-PsaL MSEFVKPFNNDPFVGNLSTPVTT
Eh-PsaL MSEFVKPYNNDPFVGNLSTPVTT
Ss-PsaL GFELLDEDEMKVAADYDKLMMEGKIPFAVPGPAGFWYTGAVIQWKGKEQFAGDQVQTLTE
α1 TM1 α2
No-PsaL SA.FTRAYLKVLPAYRPGLTPLSRGAEIGFTHGYFLIGPFYTYGPLRSVEFSLTSLAAGL
Ng-PsaL SA.FTRAYLKVLPAYRPGLTPLSRGAEIGFTHGYFLIGPFYTYGPLRSAEFSLTSLAAGL
Ns-PsaL SA.FTRAYLKVLPAYRPGLTPLSRGAEIGFTHGYFLIGPFYTYGPLRSAEFSLTSLAAGL
Te-PsaL SG.LVKTFIGNLPAYRQGLSPILRGLEVGMAHGYFLIGPWVKLGPLRDSDVAN...LGGL
Cr-PsaL AP.IVATYLSNLPAYRTGVAPVLRGVEIGLAHGFLLAGPFIKLGPLRNVPETA..EIAGS
Pp-PsaL SP.LIAWYLSNLPAYRTAVAPLLRGVEIGLAHGYLLVGPFVLAGPLRNSAVRG..EAG.S
Zm-PsaL SP.LVAWYLSNLPAYRTAVSPLLRGVEVGLAHGYLLVGPFALTGPLRSTPVHG..QAG.A
Cm-PsaL SS.LTRAYLSQLPIYRRGVSPFLRGLEIGMAHGYFLIGPFVQLGPLRNTDIKY...LAGL
Tm-PsaL SA.ATKAFLGNLPAYRAGLSPLLRGLEVGMAHGYLLVGPFDKLGPLRNSEIAL...LSGF
Cg-PsaL SA.VTRSLLKNLPAYRFGLTPLLRGLEIGLAHGYFLIGPFFKLGPLRNSEIAL...FAGF
Rs-PsaL SS.FTKSLLSNLPAYRAGLSPLLRGVEIGLTHGYFLVGPFYKLGPLRNSDVAL...LSGF
Ig-PsaL ST.ATKLYLGNLPIYRKGLSPLMRGLEVGMAHGYFLIGPFYILGPLRNSPNAL...LVGL
Eh-PsaL ST.ATKLYLGNLPIYRKGLSPLLRGLEIGMAHGYFLIGPFYILGPLRNSPNAL...LVGL
Ss-PsaL NGRFSKQFLANLAFYRDGLKPWQRGLEIGMAHGYFLIGPFTSLGPLRNTPEAAT...VGL
α3 TM2 α4
No-PsaL LAAITLLLILTVGLSIYGQVTYDVYDNALIVKLVRQMVGSERTQDLPQIKGTSELDTVLG
Ng-PsaL LAAITLLLILTVGLSIYGQVTYDVYDNALIVKLVRQMVGSEKTQELPQIKGTSELDTILG
Ns-PsaL LAAITLLLILTVGLSIYGQVTYDVYDNALIVKLVQQMVGSEKTQELPQIKGTSELDTILG
Te-PsaL ISGIALILVATACLAAYGLVSFQKGGSSS.....DPLKTSEG
Cr-PsaL LSAAGLVLILALCLSIYGSAQFQS..TPSIGVKTLS.....GRSVARDPLFSADG
Pp-PsaL LAAAGLVAILTMCLTIYGIASFKEGEASKAPSLTLT.....GRQKAADKLQTAEG
Zm-PsaL LGAAGLVAILSVCLTMYGVASFNEGDPSTAPSLTLT.....GRKKEADKLQTSDG
Cm-PsaL LSAIGLIVILTLGMLLYGAVSFTNDS.....QDLESVDG
Tm-PsaL LSAVGLITILTLCLTIYGKVSFD.....LLTEDG
Cg-PsaL LSTIGLILILTLGLTIYGAVVFKEEKVMSSANV.....NNLQTKKA
Rs-PsaL FSALGLIVILVACLTIYGVVSFEETEAK.....DQLQTAKG
Ig-PsaL FSAYGLIIILTLALTIYGLASFQDNSTG.....SNLESSKG
Eh-PsaL FSAFGLILILTLGLTIYGLASFQGTEGG.....ENLESAKG
Ss-PsaL LCGCAIVGLVSIGGLIFGSTIKPTRFDK.....EGDKPASG
α5 TM3
No-PsaL WQKFSEGFFSGGLIGSIVAAVGIALYSTYL.....
Ng-PsaL WQKFSEGFFSGGLIGSIVAAIGIALYSTYL.....
Ns-PsaL WQKFSEGFFSGGLIGSIVAAIGIALYSTYL.....
Te-PsaL WSQFTAGFFVGAMGSAFVAFFLLENFSVVDGIMTGLFN
Cr-PsaL WSEFAAGFLVGGEAGVAWAYVCTQILPYYS.....
Pp-PsaL WAGFTGGFFFGGLSGVAWAYILLYVLNLPYPVK.....
Zm-PsaL WAKFTGGFFFGGISGVLWAYFLLYVLDLPYFFK.....
Cm-PsaL WRQLASGFLLGAVGGAGFAYLLLTLFS.....
Tm-PsaL WSQFTSGFLVGAFGCAGFAYLTLLNA.....
Cg-PsaL WDQFKGGFFVGACGSAGFALICLYV.....
Rs-PsaL WRQFTSGWLVGSVGGASFAYILISNIPFLQTAGMSMLK
Ig-PsaL WRSFTSGFTVGALGGASVAYVLLNNVSFFA.....
Eh-PsaL WRNFTSGFSIGAFGGASVAYVLLDNISFFA.....
Ss-PsaL FIEMINWHAIGGLGGAGFAHALITVFGS.....

**b**

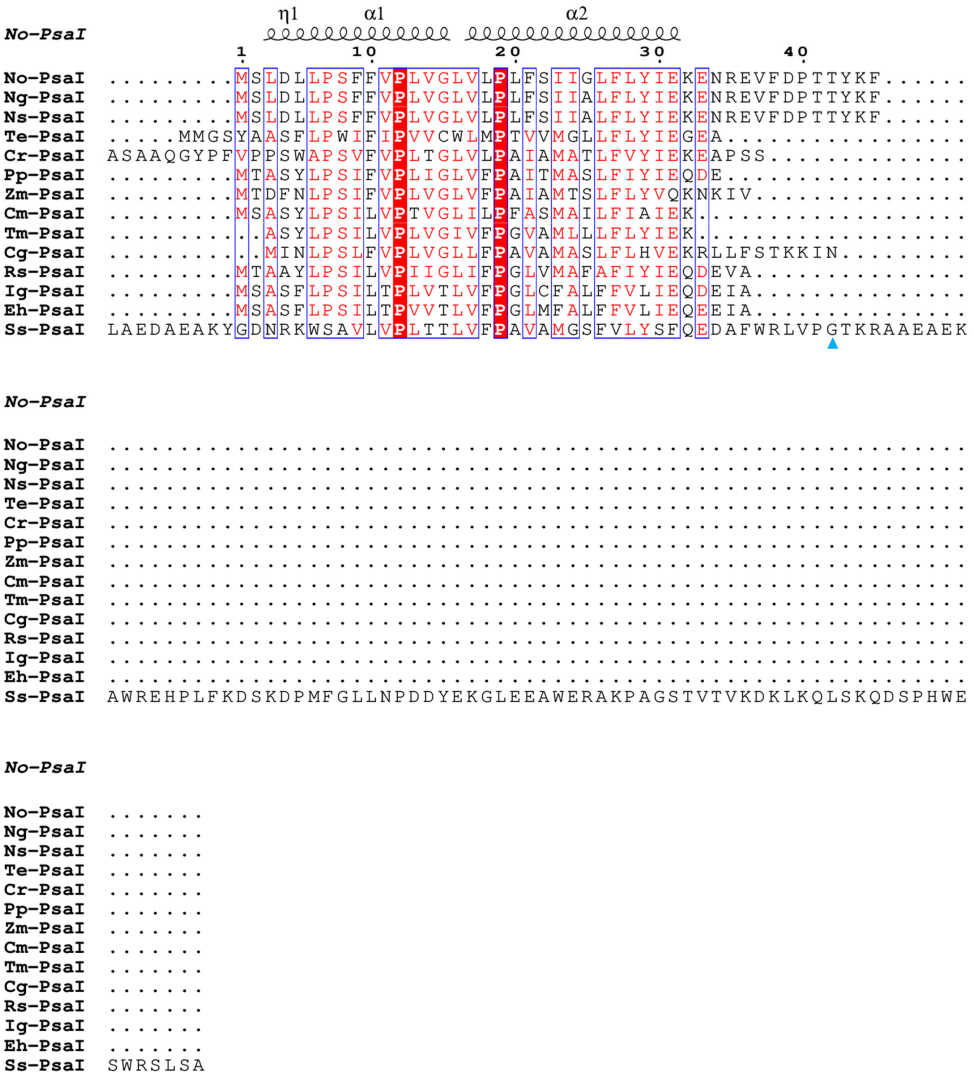


**Supplementary Fig. 3 | Sequence alignment of PsaL and PsaI across different photosynthetic organisms.**

**a, b,** Multiple sequence alignment of PsaL (**a**) and PsaI (**b**) from representative species: *N. oceanica* (No), *N. gaditana* (Ng), *N. salina* (Ns), cyanobacterium *T. elongatus* (Te), green alga *C. reinhardtii* (Cr), moss *P. patens* (Pp), vascular plant *Z. mays* (Zm), red alga *C. merolae* (Cm), xanthophyte *T. minus* (Tm), diatom *C. gracilis* (Cg), cryptophyte *R. salina* (Rs), haptophytes *I. galbana* (Ig), *E. huxleyi* (Eh), and dinoflagellate *Symbiodinium* sp. (Ss). The extended loop between TM2 and TM3 in NoPsaL is markered with a blue line. Fully conserved and similar residues are highlighted with red backgrounds and blue boxes, respectively. The unique FNR interaction residues in NoPsaL and NoPsaI are marked with blue triangles.

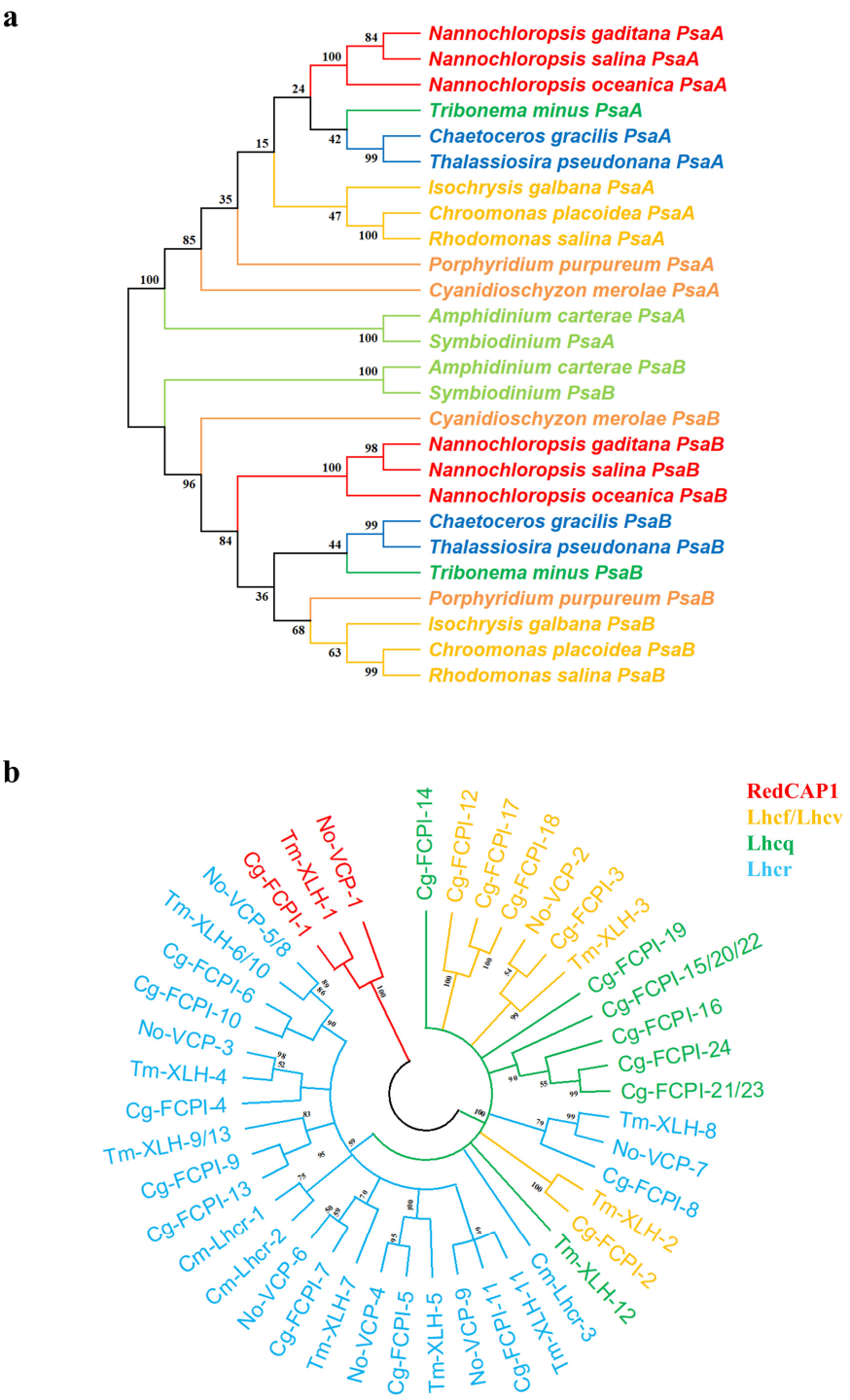


**Supplementary Fig. 4 | Phylogenetic analysis of PSI core and antenna proteins in *N. oceanica* and related red lineage species.**

**a,** Phylogenetic tree of PsaA/B core subunits from red lineage species. **b,** Phylogenetic tree of VCP antenna proteins from *N. oceanica* compared with those from xanthophyte *T. minus* (Tm), diatom *C. gracilis* (Cg), and red algae *C. merolae* (Cm). Protein clades including RedCap, Lhcf/Lhcv, Lhcq, and Lhcr are highlighted in red, yellow, green and blue, respectively. Evolutionary analyses were performed using MEGA11[1]; bootstrap values from 1000 replicates are shown at the branch nodes.

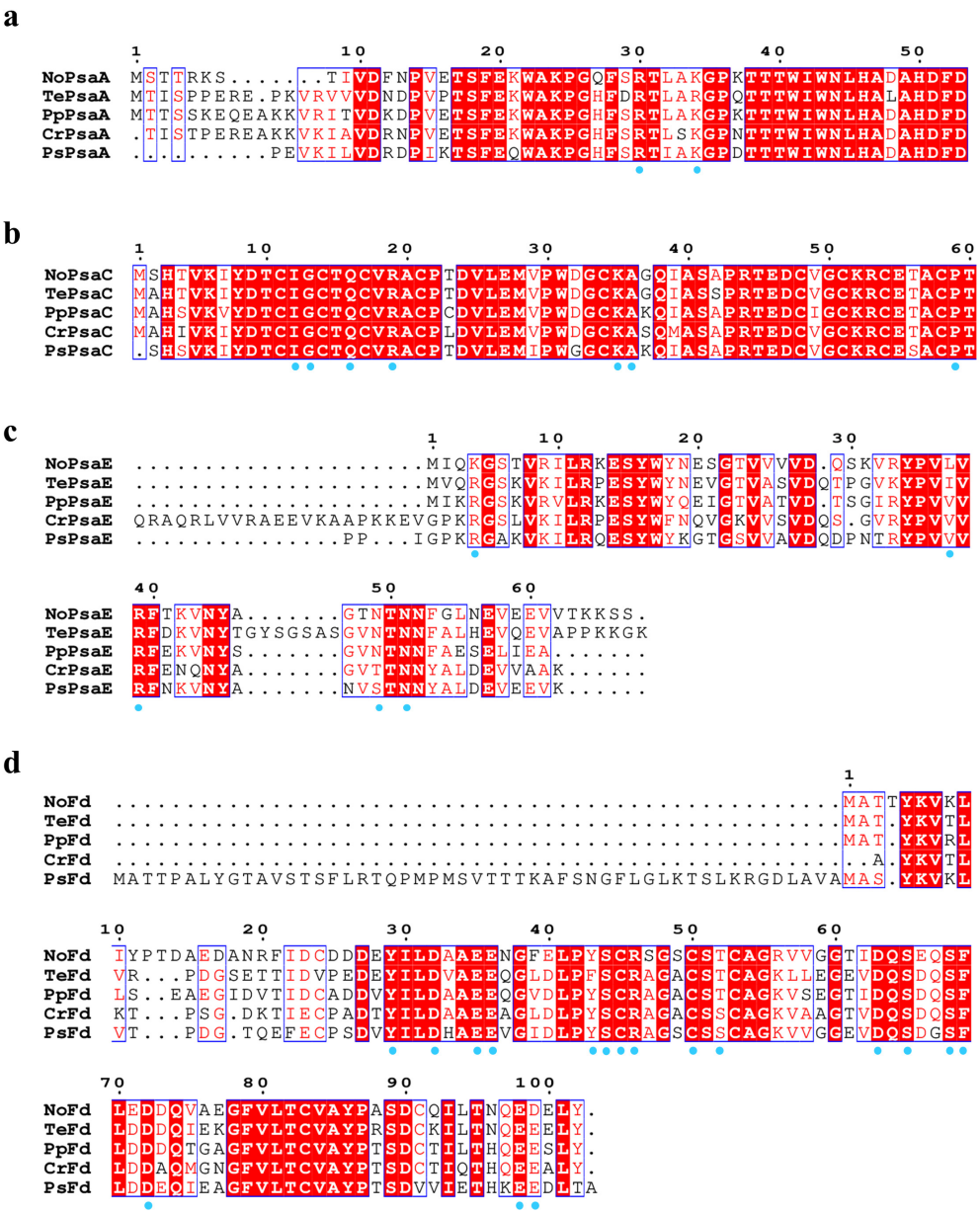


**Supplementary Fig. 5 | Sequence alignment of Fd and its interacting PSI core subunits across species.**

**a-c,** Sequence alignment of Fd-interacting PSI core subunits from *N. oceanica* (No): PsaA (**a**), PsaC (**b**), and PsaE (**c**), with their homologs from other species. **d,** Sequence alignment of NoFd with orthologs from other species. Abbreviations: *N. oceanica* (No), cyanobacterium *T. elongatus* (Te), red algae *P. purpureum* (Pp), green algae *C. reinhardtii* (Cr), and vascular plant pea *Pisum sativum* (Ps). Identical and similar residues are highlighted with red backgrounds and blue boxes, respectively. Residues involved in Fd-subunit interactions are marked with blue dots.

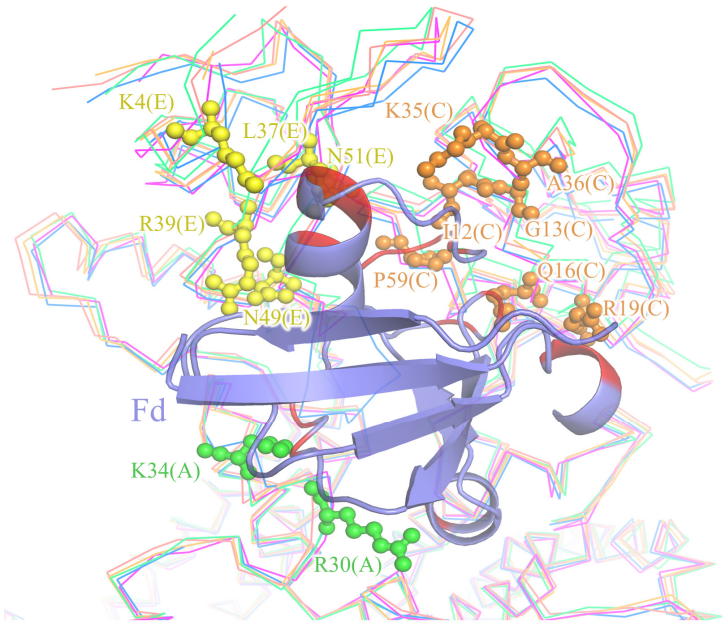


**Supplementary Fig. 6 | Structural comparison of the potential Fd-binding subunits from *N. oceanica* with those from other representative species.**

The Fd-binding subunits PsaA, PsaC, and PsaE from the cyanobacterium *T. elongatus* (Te; blue-purple), red alga *P. purpureum* (Pp; magenta), green alga *C. reinhardtii* (Cr; green), and the vascular plant *P. sativum* (Ps; orange-red) are shown as ribbons. Conserved residues involved in Fd interaction are highlighted as stick-and-ball models, with corresponding subunit labels (e.g., A for PsaA) indicated in parentheses. For clarity, only TeFd is shown in cartoon representation to illustrate the conserved Fd-binding site; its interacting residues with PsaA, PsaC, and PsaE are colored red.

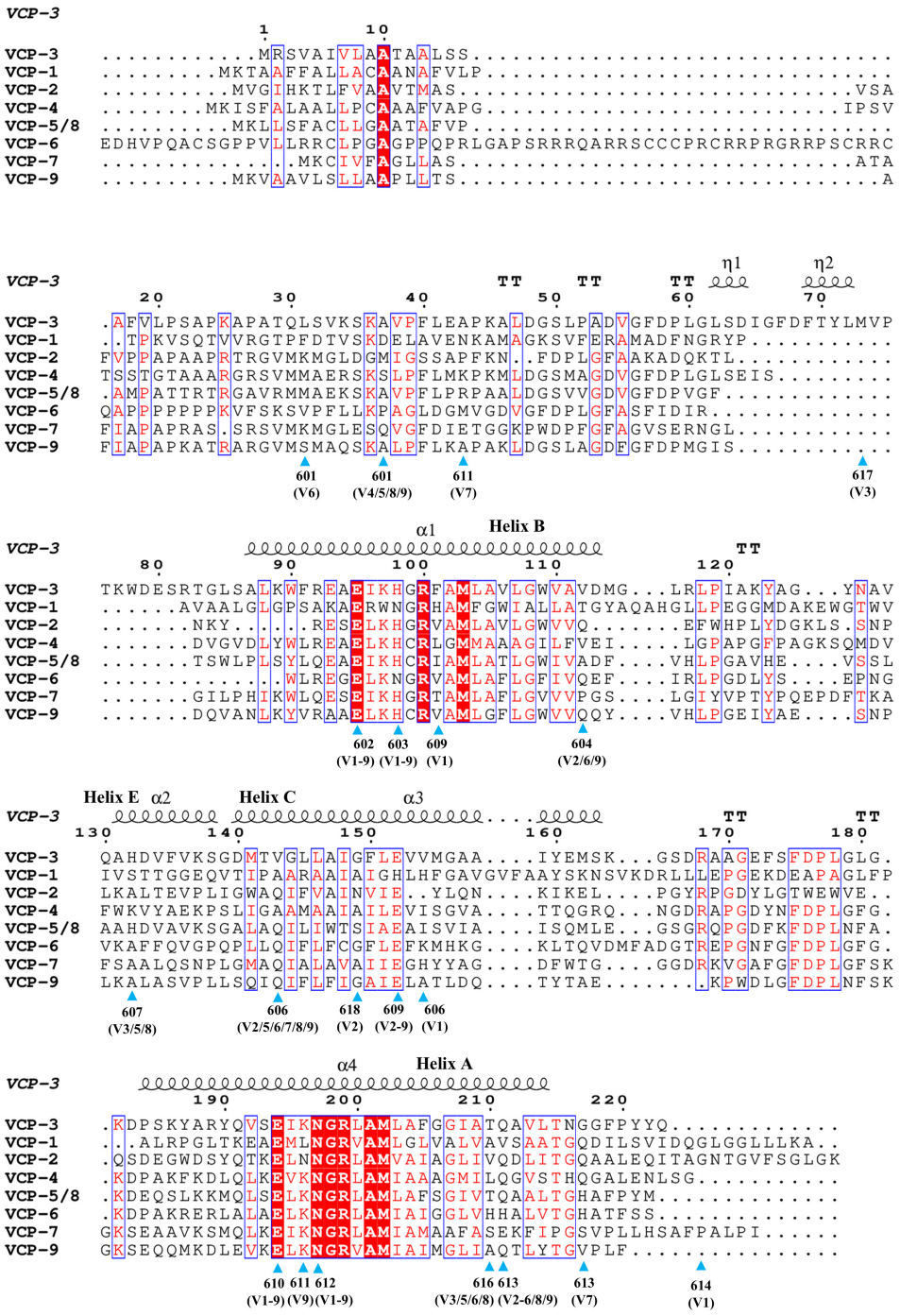


**Supplementary Fig. 7 | Sequence alignment of all VCP proteins in *N. oceanica*.** Sequence alignment of VCPs1-9. Note that VCP5 and VCP8 share an identical sequence. Secondary structure elements are shown above the alignment. Fully conserved and similar residues are highlighted with red backgrounds and blue boxes, respectively. Chlorophyll *a* (Chl *a*) coordinating residues are marked with blue triangles and labeled accordingly. The letter 'V' denotes the VCP protein.

**a**

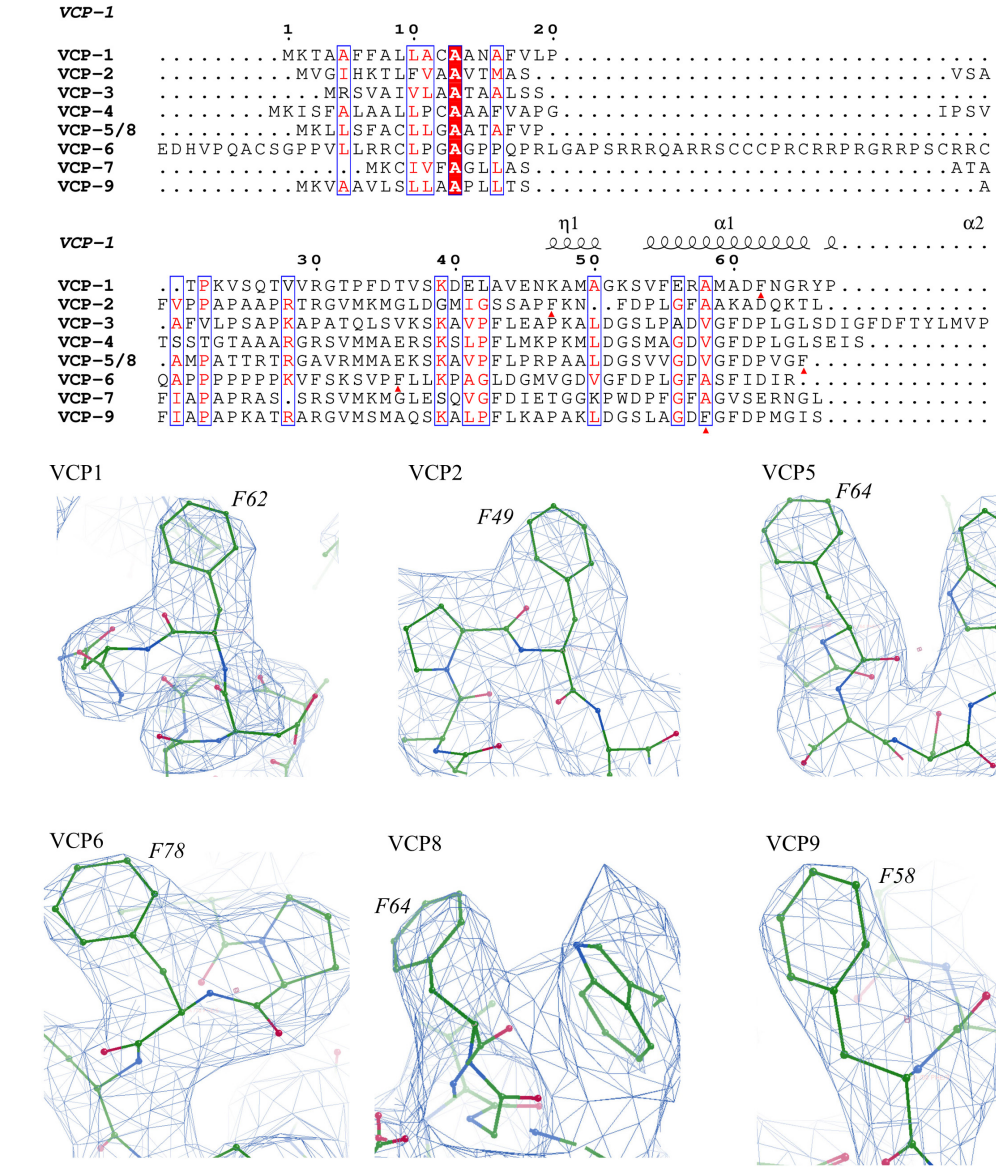
VCP-1
1 10 20
VCP-1 .....MKTAAFFALLACAANAFVLP.....
VCP-2 .....MVGIHKTLFVAAVTMAS.....VSA
VCP-3 .....MRSVAIVLAATAALSS.....
VCP-4 .....MKISFALAALLPCAAAFVAPG.....IPSV
VCP-5/8 .....MKLLSFACLLGAATAFVP.....
VCP-6 EDHVPQACSGPPVLLRRCLPGAGPPQPRLGAPSRRRQARRSCCCPRCRRPRGRRPSCRRC
VCP-7 .....MKCIVFAGLLAS.....ATA
VCP-9 .....MKVAAVLSLLAAPLLTS.....A
η1 α1 α2
VCP-1
30 40 50 60
VCP-1 ..TPKVSQTVVRGTPFDTVSKDELAVENKAMAGKSVFERAMADFNGRYP.....
VCP-2 FVPPAPAAPRTRGVMKMGLDGMIGSSAPFKN..FDPLGFAAKADQKTL.....
VCP-3 .AFVLPSAPKAPATQLSVKSKAVPFLEAPKALDGSLPADVGFDPLGLSDIGFDFTYLMVP
VCP-4 TSSTGTAAARGRSVMMAERSKSLPFLMKPKMLDGSMAGDVGFDPLGLSEIS.....
VCP-5/8 .AMPATTRTRGAVRMMAEKSKAVPFLPRPAALDGSVVGDVGFDPVGF.....
VCP-6 QAPPPPPPPKVFSKSVPFLLKPAGLDGMVGDVGFDPLGFASFIDIR.....
VCP-7 FIAPAPRAS..SRSVMKMGLESQVGFDIETGGKPWDPFGFAGVSERNGL.....
VCP-9 FIAPAPKATRARGVMSMAQSKALPFLKAPAKLDGSLAGDFGFDPMGIS.....
VCP1
F62
VCP2
F49
VCP5
F64
VCP6
F78
VCP8
F64
VCP9
F58

**b**

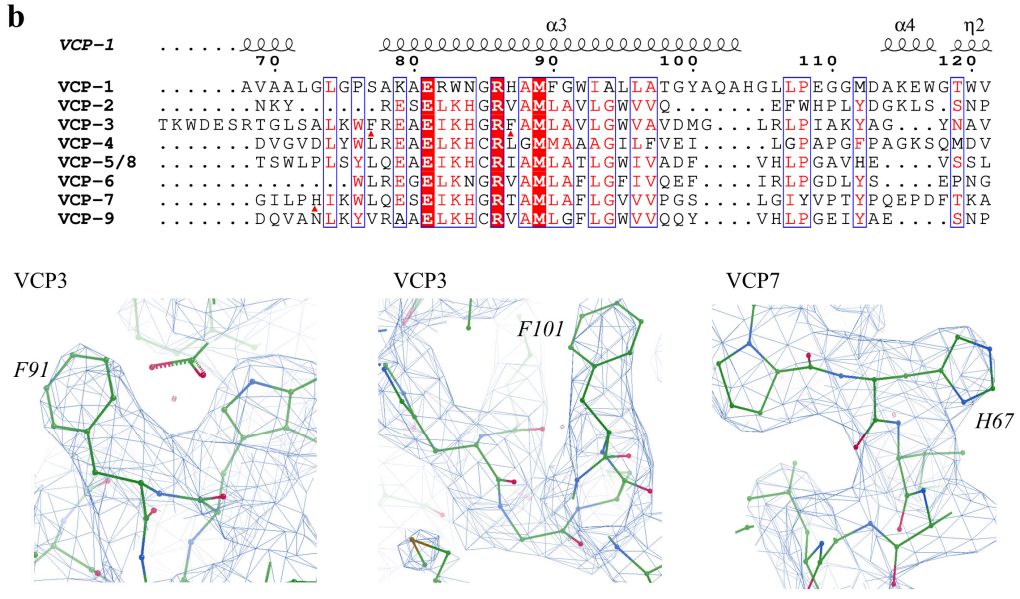
α3 α4 η2
VCP-1 ..... 70 80 90 100 110 120
VCP-1 .....AVAALGLGPSAKAERWNGRHAMFGWIALLATGYAQAHGLLPEGGMDAKEWGTWV
VCP-2 .....NKY.....RESELKHGRVAMLAVLGWVVQ.....EFWHPLYDGKLS.SNP
VCP-3 TKWDESRTGLSALKWFREAEIKHGRFAMLAVLGWVAVDMG...LRLPIAKYAG...YNAV
VCP-4 .....DVGVDLYWLREAELKHCRLGMMAAAGILFVEI.....LGPAPGFPAGKSQMDV
VCP-5/8 .....TSWLPLSYLQEAEIKHCRIAMLATLGWIVADF....VHLPGAVHE....VSSL
VCP-6 .....WLREGELKNGRVAMLAFLGFIVQEF....IRLPGDLYS....EPNG
VCP-7 .....GILPHIKWLQESEIKHGRTAMLAFLGVVVPGS....LGIYVPTYPQEPDFTKA
VCP-9 .....DQVANLKYVRAAELKHCRVAMLGFLGWVVQQY....VHLPGEIYAE....SNP
VCP3
F91
VCP3
F101
VCP7
H67

**c**

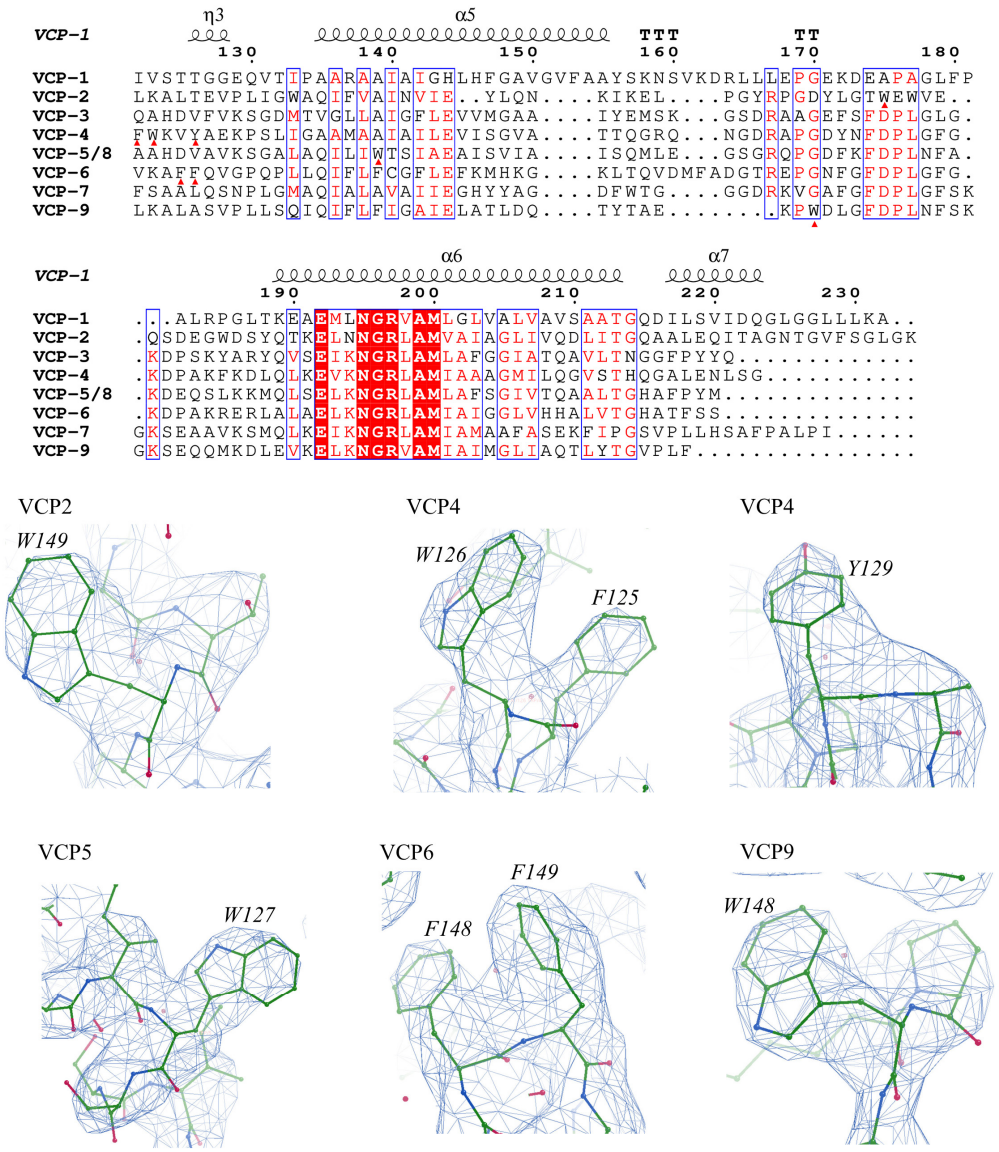


**Supplementary Fig. 8 | Identification of individual VCP proteins by characteristic residue densities.**

(**a-c**) Cryo-EM density maps and corresponding sequence segments for each VCP. Residues are numbered according to VCP1. Fully conserved and similar residues are shaded in red and boxed in blue, respectively. Unique residues used for identification are marked with red triangles, and the corresponding cryo-EM densities are displayed below and labeled in italics.

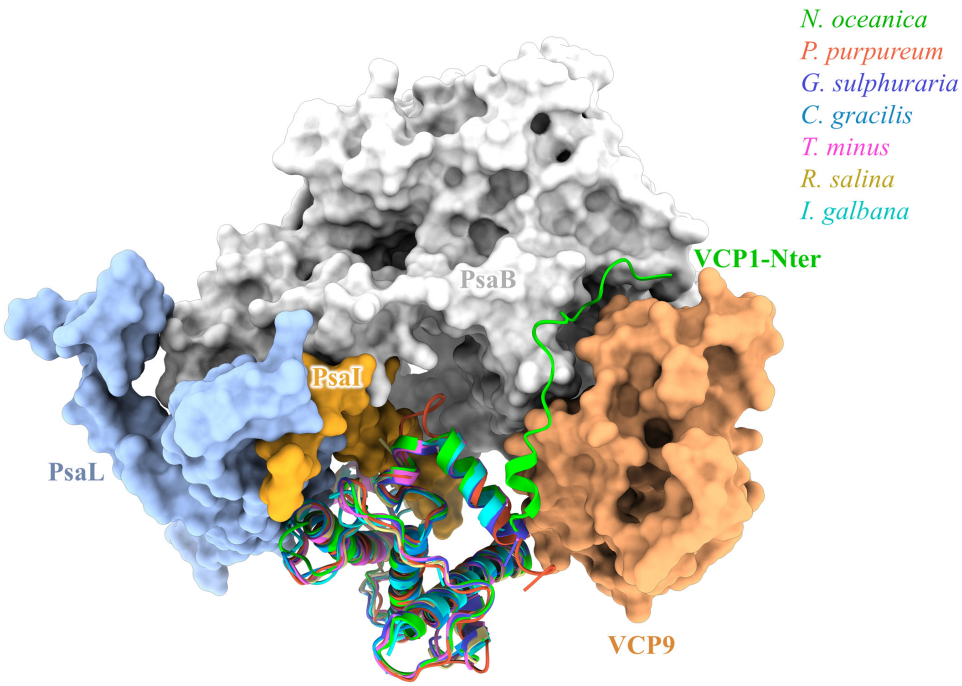


**Supplementary Fig. 9 | Structural comparison of NoVCP1 (RedCap) with its homologs from red lineage algae.**

VCP1 and its homologs from various species are shown in cartoon. The surrounding subunits of VCP1 in *N. oceanica* are depicted as surface. The compared RedCap structures include those from red algae *P. purpureum* (7Y5E) and *G. sulphuraria* (9KC5), diatom *C. gracilis* (6LY5), xanthophyte *T. minus* (9M4F), cryptophytes *R. salina* (8WM6) and haptophyte *I. galbana* (8Z11).

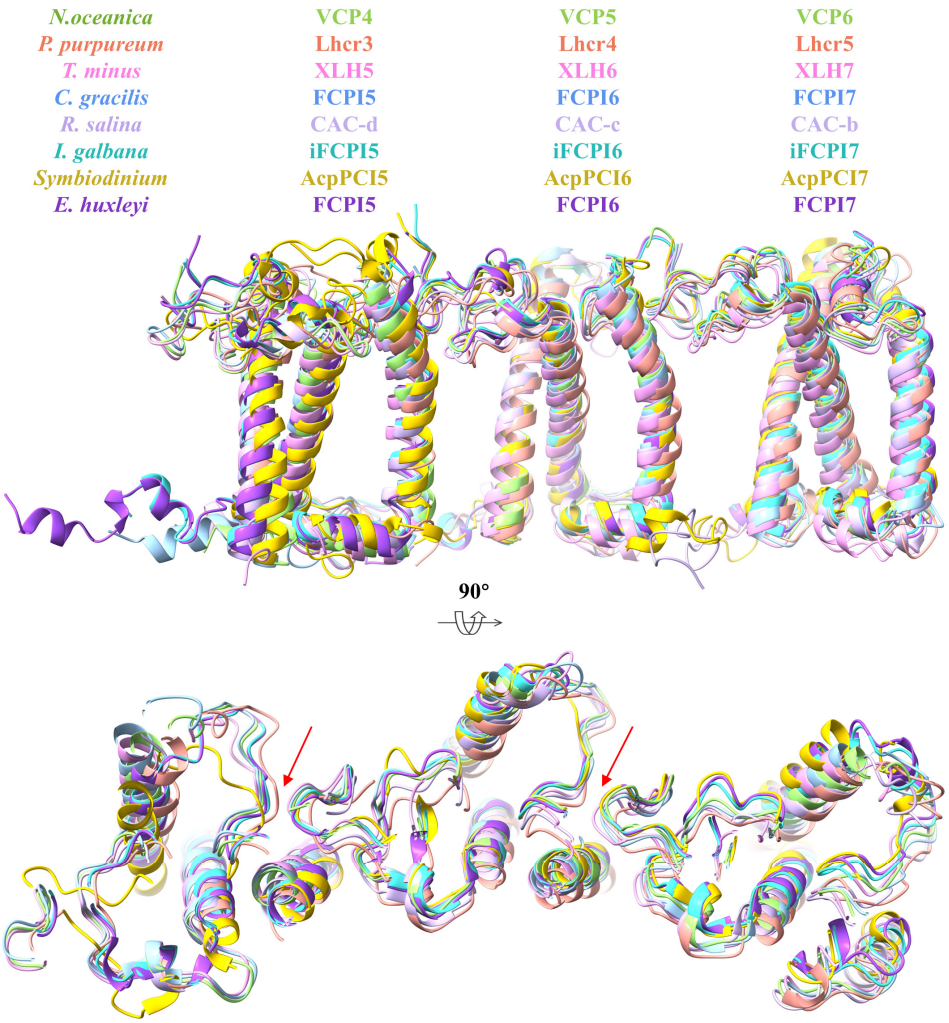


**Supplementary Fig. 10 | Structural comparison of trimeric light-harvesting complex apoproteins.**

Structural superposition of the VCP4/5/6 trimer with homologous trimers from red alga *P. purpureum* (Lhcrs3/4/5; 7Y5E), xanthophyte *T. minus* (XLHs5/6/7; 9M4F), diatom *C. gracilis* (FCPIs-5/6/7; 6LY5), cryptophyte *R. salina* (CACs-d/c/b; 8WM6), haptophyte *I. galbana* (iFCPIs-5/6/7; 8Z11), dinoflagellate *Symbiodinium* sp. (AcpPCIs-5/6/7; 8JJR), and coccolithophore *E. huxleyi* (FPCIs-5/6/7; 9JJ8). Each trimer is shown in a distinct color. Red arrows indicate loops involved in trimer interactions.

**Supplementary Table 1 | Summary of the structural model of NoPSI-VCP-FNR supercomplex**

| Subunits | Chains | Total (Traced) residues | Chl *a* | Cars | Lipids | Other ligands |
|---|---|---|---|---|---|---|
| PsaA | A | 745 (7-745) | 42 | 6 Bcr | 6 PG, 2 MGDG | 1 PQN |
| PsaB | B | 737 (2-737) | 42 | 8 Bcr | 3 PG | 1 PQN,1 SF4 |
| PsaC | C | 81 (2-81) | | | | 2 SF4 |
| PsaD | D | 136 (3-133) | | | | |
| PsaE | E | 67 (2-61) | | | | |
| PsaF | F | 185 (24-185) | 3 | 2 Bcr | 1 PG | |
| PsaI | I | 45 (1-42) | 1 | 2 Bcr | 1 MGDG | |
| PsaJ | J | 41 (1-41) | 2 | 2 Bcr | 1 MGDG | |
| PsaL | L | 172 (2-172) | 3 | | 2 PG | |
| PsaM | M | 30 (1-30) | | 1 Bcr | | |
| PsaR | R | 128 (45-128) | 2 | 1 Vio | | |
| FNR | f | 412(40-92, 104-412) | | | | 1 FAD |
| VCP1 | 1 | 232 (31-228) | 8 | 2 Bcr, 3 Vio | | |
| VCP2 | 2 | 208 (38-202) | 10 | 2 Vio, 2 Vau | | |
| VCP3 | 3 | 223 (38-220) | 13 | 1 Bcr, 3 Vio, 1 Vau | 1 MGDG | |
| VCP4 | 4 | 220 (43-219) | 9 | 5 Vio | 2 PG, 1 MGDG | |
| VCP5 | 5 | 202 (35-202) | 12 | 5 Vio | 2 PG, 1 MGDG | |
| VCP6 | 6 | 240 (69-239) | 11 | 1 Bcr, 4 Vio | | |
| VCP7 | 7 | 213 (34-212) | 9 | 1 Bcr, 4 Vio | | |
| VCP8 | 8 | 202 (37-200) | 12 | 2 Bcr, 3 Vio | | |
| VCP9 | 9 | 199 (36-199) | 10 | 1 Bcr, 2 Vio, 1 Vau | | |
| Total | 21 | 4718 (4207) | 189 | 29 Bcr, 32 Vio, 4 Vau | 16 PG, 7 MGDG | 2 PQN, 3 SF4, 1 FAD |

Chl *a*, chlorophyll *a*; Car, carotenoid; Bcr, β-carotene; Vio, violaxanthin; Vau, vaucheriaxanthin; PG, phosphatidyl glycerol; MGDG, monogalactosyldiacyl glycerol; PQN, phylloquinone; SF4, sulphur-iron cluster; FAD, flavin adenine dinucleotide.

**Supplementary Table 2 | Comparison of protein subunits in the PSI-LHCI supercomplex from *N. oceanica* and other organisms.**

| Subunits | *N.oceanica* | Red alga | Xanthophyte | Diatom | Cryptophyte | Haptophyte | Coccolithophore | Dinoflagellate | Green alga | Moss | Land plant |
|---|---|---|---|---|---|---|---|---|---|---|---|
| PsaA | √ | √ | √ | √ | √ | √ | √ | √ | √ | √ | √ |
| PsaB | √ | √ | √ | √ | √ | √ | √ | √ | √ | √ | √ |
| PsaC | √ | √ | √ | √ | √ | √ | √ | √ | √ | √ | √ |
| PsaD | √ | √ | √ | √ | √ | √ | √ | √ | √ | √ | √ |
| PsaE | √ | √ | √ | √ | √ | √ | √ | √ | √ | √ | √ |
| PsaF | √ | √ | √ | √ | √ | √ | √ | √ | √ | √ | √ |
| PsaG | | | | | | | | | √ | √ | √ |
| PsaH | | | | | | | | | √ | √ | √ |
| PsaI | √ | √ | √ | √ | √ | √ | √ | √ | √ | √ | √ |
| PsaJ | √ | √ | √ | √ | √ | √ | √ | √ | √ | √ | √ |
| PsaK | | √ | | | √ | √ | √ | | √ | √ | √ |
| PsaL | √ | √ | √ | √ | √ | √ | √ | √ | √ | √ | √ |
| PsaM | √ | √ | √ | √ | √ | √ | √ | √ | √ | √ | |
| PsaN | | | | | | | | | √ | | √ |
| PsaO | | √ | | | √ | | | | √ | √ | √ |
| PsaQ | | | | | √ | | | | | | |
| PsaR | √ | √ | √ | √ | √ | √ | √ | √ | | | |
| PsaS | | | √ | √ | | | | | | | |
| PsaT | | | | | | | | √ | | | |
| PsaU | | | | | | | | √ | | | |
| PsaX | | | | | | | | | | | |
| ACPI-S | | | | | √ | | | | | | |
| LHCI | 9 | 3, 5, 7 or 8 | 13 | 13, 16 or 24 | 11 or 14 | 22 | 38 | 12, 13, 14 or 18 | 6, 8 or 10 | 4 or 8 | 4 |

The symbol "√" indicates the presence of the subunit. The subunit composition of each species is as reported in the following references: red alga[2-4]; xanthophyte[5]; diatom[6-8]; cryptophyte[9,10]; haptophyte[11]; coccolithophore[12]; dinoflagellate[13,14]; green alga[15-20], moss[21-24], and vascular plant[25,26].

**Supplementary Table 3 | Pigment Binding sites in VCP subunits and their comparison with equivalent from xanthophyte and diatom.**

| Subunits/ Sites | VCP1/ XLH1/ FCPI-1 | VCP2/ XLH3/ FCPI-3 | VCP3/ XLH4/ FCPI-4 | VCP4/ XLH5/ FCPI-5 | VCP5/ XLH6/ FCPI-6 | VCP6/ XLH7/ FCPI-7 | VCP7/ XLH8/ FCPI-8 | VCP8/ XLH10/ FCPI-10 | VCP9/ XLH11/ FCPI-11 |
|---|---|---|---|---|---|---|---|---|---|
| 601 | - | - | Chl *a*/*a*/*a* | Chl *a*/*a*/*a* (S47) | Chl *a*/*a*/*a* (A39) | Chl *a*/*a*/*a* (V76) | - | Chl *a*/*a*/*a* | Chl *a*/*a*/*a* (A40) |
| 602 | Chl *a*/*a*/*a* (E81) | Chl *a*/*a*/*a* (E73) | Chl *a*/*a*/*a* (E95) | Chl *a*/*a*/*a* (E89) | Chl *a*/*a*/*a* (E77) | Chl *a*/*a*/*a* (E112) | Chl *a*/*a*/*a* (E75) | Chl *a*/*a*/*a* (E77) | Chl *a*/*a*/*a* (E79) |
| 603 | Chl *a*/*a*/*a* (N84) | Chl *a*/*a*/*a* (H76) | Chl *a*/*a*/*a* (H98) | Chl *a*/*a*/*a* (H92) | Chl *a*/*a*/*a* (H80) | Chl *a*/*a*/*a* (N115) | Chl *a*/*a*/*a* (H78) | Chl *a*/*a*/*a* (H80) | Chl *a*/*a*/*a* (H82) |
| 604 | - | Chl *a*/*a*/*a* (Q90) | Chl *a*/*a*/*a* | Chl *a*/-/- | Chl *a*/*a*/*a* | Chl *a*/*a*/*a* (Q129) | Chl *a*/*a*/*a* | Chl *a*/*a*/*a* | Chl *a*/*a*/*a* (Q96) |
| 606 | Chl *a*/*a*/*a* (H146) | Chl *a*/*a*/*a* (Q119) | - | - | Chl *a*/*a*/*a* (Q123) | Chl *a*/*a*/*a* (Q158) | Chl *a*/*a*/*a* (Q125) | Chl *a*/*a*/*a* (Q123) | Chl *a*/*a*/*a* (Q125) |
| 607 | Chl *a*/*a*/*a* | - | Chl *a*/*a*/*a* (H132) | - | Chl *a*/*a*/*a* (H112) | - | - | Chl *a*/*a*/*a* (H112) | - |
| 608 | - | - | - | - | - | - | - | - | -/Chl *a*/- |
| 609 | Chl *a*/*a*/*a* (H87) | Chl *a*/*a*/*a* (E128) | Chl *a*/*a*/*a* (E152) | Chl *a*/*a*/*a* (E147) | Chl *a*/*a*/*a* (E132) | Chl *a*/*a*/*a* (E167) | Chl *a*/*a*/*a* (E134) | Chl *a*/*a*/*a* (E132) | Chl *a*/*a*/*a* (E134) |
| 610 | Chl *a*/*a*/*a* (E192) | Chl *a*/*a*/*a* (E166) | Chl *a*/*a*/*a* (E194) | Chl *a*/*a*/*a* (E189) | Chl *a*/*a*/*a* (E174) | Chl *a*/*a*/*a* (E212) | Chl *a*/*a*/*a* (E177) | Chl *a*/*a*/*a* (E174) | Chl *a*/*a*/*a* (E173) |
| 611 | - | Chl *a*/*a*/*a* | Chl *a*/*a*/*c* | Chl *a*/*a*/*c* | Chl *a*/*a*/*a* | Chl *a*/*a*/*a* | Chl *a*/*a*/*a* (E42) | Chl *a*/*a*/*a* | Chl *a*/*a*/*a* (K175) |
| 612 | Chl *a*/*a*/*c* (N195) | Chl *a*/*a*/*a* (N169) | Chl *a*/*a*/*a* (N197) | Chl *a*/*a*/*a* (N192) | Chl *a*/*a*/*c* (N177) | Chl *a*/*a*/*c* (N215) | Chl *a*/*a*/*c* (N180) | Chl *a*/*a*/*c* (N177) | Chl *a*/*a*/*c* (N176) |

| | | | | | | | | | |
|---|---|---|---|---|---|---|---|---|---|
| 613 | - /Chl *a*/- | Chl *a*/*a*/*a* (Q183) | Chl *a*/*a*/*a* (Q211) | Chl *a*/-/- (Q206) | Chl *a*/*a*/*a* (Q191) | Chl *a*/*a*/*a* (H229) | Chl *a*/*a*/*a* (S200) | Chl *a*/*a*/*a* (Q191) | Chl *a*/*a*/*a* (Q190) |
| 614 | Chl *a*/*a*/- (G224) | - | - | - | - | - | - | - | - |
| 615 | - | - | | - | - | - | - | - | - |
| 616 | - | - | Chl *a*/*a*/*a* (T210) | - | Chl *a*/*a*/*a* (T190) | Chl *a*/*a*/*a* (H228) | - | Chl *a*/*a*/*a* (T190) | - |
| 617 | - | - | Chl *a*/*a*/*a* (M73) | - | - | - | - | - | - |
| 618 | - | Chl *a*/-/- (N125) | Chl *a*/Chl *a*/- | - | - | -/Chl *a*/- | - | - | - |
| 621 | Bcr/Bcr/Fx | Vau/Vau/Fx | Vio/Ddx/Fx | Vio/Ddx/Fx | Vio/Ddx/Ddx | Vio/Ddx/Ddx | Vio/Ddx/ Fx | Vio/Ddx/Ddx | Vio/Ddx/Ddx |
| 622 | Vio/Ddx/Ddx | Vio/Ddx/Ddx | Vio/Ddx/Ddx | Vio/Ddx/Ddx | Vio/Ddx/Ddx | Vio/Vau/ Ddx | Vio/Ddx/Ddx | Vio/Ddx/Ddx | Vio/Ddx/Ddx |
| 623 | - | Vau/Ddx/Fx | Bcr/Ddx/Fx | Vio/-/- | Vio/Ddx/Ddx | Vio/Ddx/Ddx | Vio/Ddx/ Fx | Bcr/Ddx/Fx | - |
| 624 | Vio/Ddx/Fx | Vio/Ddx/Fx | Vio/Ddx/Fx | Vio/-/- | Vio/Ddx/Fx | Vio/Ddx/Fx | Bcr/Ddx/Ddx | Bcr/Ddx/Fx | Bcr/Ddx/- |
| 625 | - | - | Vau/Bcr/Fx | Vio/-/- | Vio/Ddx/Ddx | Bcr/Bcr/Ddx | Vio/-/- | Vio/Ddx/Fx | - |
| 626 | Vio/Ddx/Ddx | - | - | - | - | - | - | - | - |
| 627 | - | - | - | - | - | - | - | - | Vau/Bcr/Fx |
| 628 | Bcr/Bcr/- | - | - | - | - | - | - | - | - |

The red characters indicate the sites that are absent in XLHs from xanthophyte *T. minus* (PDB code:9M4F) and FCPIs from diatom *C. gracilis* (PDB code:6LY5). Labels in parentheses provide annotations for the residues coordinated with chlorophyll *a*. Chl *a*, chlorophyll *a*; Chl *c*, chlorophyll *c*; Car, carotenoid; Bcr, β-carotene; Vio violaxanthin; Vau, vaucheriaxanthin; Ddx, Diadinoxanthin; Fx, fucoxanthin.

**Supplementary Table 4 | Calculated FRET rates for the excitation transfer from VCPs to the core subunits and between adjacent VCPs within 20 ps.**

| Stromal side | | | |
|---|---|---|---|
| **VCP↔VCP** | **Distance (Å)** | **FRET rate, $K_{FRET}$ ($ps^{-1}$)** | **Lifetime, τ (ps)** |
| 4-609↔5-601 | 19.7 | 0.059 | 17.094 |
| 4-610↔5-601 | 17.6 | 0.509 | 1.964 |
| 5-610↔6-601 | 16.9 | 0.723 | 1.383 |
| 8-610↔9-601 | 17.2 | 0.703 | 1.423 |
| **VCP→Core** | **Distance (Å)** | **FRET rate, $K_{FRET}$ ($ps^{-1}$)** | **Lifetime, τ (ps)** |
| 2-610→PsaA-822 | 21.8 | 0.114 | 8.760 |
| 2-610→PsaA-841 | 13.0 | 0.076 | 13.190 |
| 2-611→PsaA-822 | 22.0 | 0.064 | 15.636 |
| 2-612→PsaA-822 | 18.0 | 0.367 | 2.722 |
| 3-617→PsaA-811 | 21.3 | 0.124 | 8.078 |
| 3-617→PsaA-819 | 13.9 | 0.159 | 6.283 |
| 3-617→PsaA-821 | 16.6 | 0.774 | 1.293 |
| 4-603→PsaA-819 | 17.8 | 0.051 | 19.433 |
| 4-609→PsaA-811 | 19.1 | 0.075 | 13.388 |
| 7-609→PsaR-203 | 12.1 | 1.217 | 0.822 |
| 8-603→PsaB-822 | 22.1 | 0.065 | 15.362 |
| 8-603→PsaB-853 | 20.5 | 0.203 | 4.916 |
| 8-609→PsaB-814 | 21.1 | 0.201 | 4.986 |
| 8-609→PsaB-853 | 14.0 | 1.859 | 0.538 |
| 9-602→PsaB-813 | 18.2 | 0.215 | 4.651 |

| | | | |
|---|---|---|---|
| 9-602→PsaB-814 | 17.1 | 0.077 | 12.925 |
| 9-603→PsaB-813 | 13.6 | 0.409 | 2.446 |
| 9-603→PsaB-814 | 16.3 | 0.150 | 6.683 |
| 9-609→PsaB-813 | 15.7 | 0.152 | 6.589 |
| **Luminal side** | | | |
| **VCP↔VCP** | **Distance (Å)** | **FRET rate, $K_{FRET}$ ($ps^{-1}$)** | **Lifetime, τ (ps)** |
| 1-614↔9-606 | 20.3 | 0.065 | 15.369 |
| 3-607↔4-613 | 22.1 | 0.102 | 9.767 |
| 4-604↔5-613 | 20.6 | 0.064 | 15.687 |
| 5-606↔6-613 | 8.9 | 0.192 | 5.211 |
| 5-606↔6-616 | 14.9 | 0.370 | 2.700 |
| 6-606↔7-613 | 11.8 | 1.466 | 0.682 |
| 8-606↔9-613 | 8.8 | 4.964 | 0.201 |
| **VCP→Core** | **Distance (Å)** | **FRET rate, $K_{FRET}$ ($ps^{-1}$)** | **Lifetime, τ (ps)** |
| 1-606→PsaI-102 | 17.6 | 0.128 | 7.808 |
| 1-607→PsaI-102 | 11.9 | 2.928 | 0.342 |
| 2-606→PsaL-206 | 9.7 | 3.757 | 0.266 |
| 5-607→PsaJ-106 | 20.2 | 0.133 | 7.522 |
| 5-616→PsaA-815 | 14.3 | 0.210 | 4.753 |
| 8-607→PsaB-818 | 21.5 | 0.056 | 17.946 |
| **Transmembrane** | | | |
| **VCP↔VCP** | **Distance (Å)** | **FRET rate, $K_{FRET}$ ($ps^{-1}$)** | **Lifetime, τ (ps)** |
| 3-609↔4-601 | 19.6 | 0.132 | 7.572 |
| 3-618↔4-602 | 18.6 | 0.083 | 11.992 |
| 3-618↔4-603 | 12.4 | 0.458 | 2.186 |
| 5-606↔6-601 | 20.2 | 0.076 | 13.144 |
| 5-606↔6-603 | 23.7 | 0.076 | 13.087 |

| | | | |
|---|---|---|---|
| 5-606↔6-611 | 23.0 | 0.088 | 11.335 |
| 5-606↔6-612 | 25.2 | 0.056 | 17.808 |
| 5-609↔6-616 | 24.8 | 0.052 | 19.376 |
| **VCP→Core** | **Distance (Å)** | **FRET rate, $K_{FRET}$ ($ps^{-1}$)** | **Lifetime, τ (ps)** |
| 1-603→PsaI-102 | 16.9 | 0.253 | 3.948 |
| 1-609→PsaI-102 | 15.6 | 0.374 | 2.672 |
| 2-606→PsaL-204 | 17.7 | 0.306 | 3.271 |
| 2-606→PsaL-205 | 19.0 | 0.232 | 4.307 |
| 2-618→PsaL-206 | 20.8 | 0.256 | 3.902 |
| 3-609→PsaA-819 | 24.7 | 0.064 | 15.675 |
| 4-603→PsaA-814 | 18.6 | 0.116 | 8.630 |
| 7-603→PsaB-841 | 22.4 | 0.157 | 6.357 |
| 7-603→PsaF-205 | 19.2 | 0.054 | 18.436 |
| 7-609→PsaB-841 | 17.8 | 0.085 | 11.723 |
| 7-609→PsaR-202 | 17.3 | 0.394 | 2.539 |

The letters "1-606" represent Chl *a*606 of VCP1, while the other letters are similarly designated.

**Supplementary Table 5 | The potential excitation energy transfer (EET) pathways from VCPs to the core subunits and between adjacent VCPs.**

| Stromal EET | Luminal EET | Tr*a*nsmembrane EET |
|---|---|---|
| VCP2: Chl *a*610→PsaA: Chl *a*822/ *a*841 | VCP1: Chl *a*606/ *a*607→PsaI: Chl *a*102 | VCP1: Chl *a*603-*a*609→PsaI: Chl *a*102 |
| VCP2: Chl *a*611/ *a*612→PsaA: Chl *a*822 | VCP1: Chl *a*614→VCP9: Chl *a*606 | VCP2: Chl *a*606→PsaL: Chl *a*204/ *a*205 |
| VCP3: Chl *a*617→PsaA: Chl *a*811/ *a*819/ *a*821 | VCP2: Chl *a*606→PsaL: Chl *a*206 | VCP2: Chl *a*618→PsaL: Chl *a*206 |
| VCP4: Chl *a*603→PsaA: Chl *a*819 | VCP3: Chl *a*607→VCP4: Chl *a*613 | VCP3: Chl *a*609↔ PsaA: Chl *a*819 |
| VCP4: Chl *a*609→PsaA: Chl *a*811 | VCP4: Chl *a*604→VCP5: Chl *a*613 | VCP3: Chl *a*609 ↔VCP4: Chl *a*601 |
| VCP4: Chl *a*609/ *a*610↔VCP5: Chl *a*601 | VCP5: Chl *a*606↔VCP6: Chl *a*613/ *a*616 | VCP3: Chl *a*618↔VCP4: Chl *a*602/ *a*603 |
| VCP5: Chl *a*610↔VCP6: Chl *a*601 | VCP5: Chl *a*607→PsaJ: Chl *a*106 | VCP4: Chl *a*603→PsaA: Chl *a*814 |
| VCP7: Chl *a*609→PsaR: Chl *a*203 | VCP5: Chl a616→PsaA: Chl *a*815 | VCP5: Chl *a*606→VCP6: Chl *a*601/ *a*603/*a*611/ *a*612 |
| VCP8: Chl *a*603-*a*609→PsaB: Chl *a*853 | VCP6: Chl *a*606↔VCP7: Chl *a*613 | VCP5: Chl *a*609→VCP6: Chl *a*616 |
| VCP8: Chl *a*603↔PsaB: Chl *a*822 | VCP8: Chl *a*606↔VCP9: Chl *a*613 | VCP7: Chl *a*603→PsaF: Chl *a*205 |
| VCP8: Chl *a*609↔ PsaB: Chl *a*814 | VCP8: Chl *a*607↔ PsaB: Chl *a*818 | VCP7: Chl *a*609→PsaR: Chl *a*202 |
| VCP8: Chl *a*610↔VCP9: Chl *a*601 | | VCP7: Chl *a*603/ *a*609→Ps*a*B: Chl *a*841 |
| VCP9: Chl *a*602/ *a*603→PsaB: Chl *a*813/ *a*814 | | |
| VCP9: Chl *a*609→PsaB: Chl *a*813 | | |

**References**


1 Tamura, K., Stecher, G., Kumar, S. & Battistuzzi, F. U. MEGA11: Molecular Evolutionary Genetics Analysis Version 11. *Molecular Biology and Evolution* **38**, 3022-3027, doi:10.1093/molbev/msab120 (2021).

2 Pi, X. *et al.* Unique organization of photosystem I–light-harvesting supercomplex revealed by cryo-EM from a red alga. *Proceedings of the National Academy of Sciences* **115**, 4423-4428, doi:10.1073/pnas.1722482115 (2018).

3 You, X. *et al.* In situ structure of the red algal phycobilisome-PSII-PSI-LHC megacomplex. *Nature* **616**, 199-206, doi:10.1038/s41586-023-05831-0 (2023).

4 Koji Kato, M. K., Yoshiki Nakajima, Takehiro Suzuki, Naoshi Dohmae, Jian-Ren Shen, Kentaro Ifuku, Ryo Nagao. Structure of a photosystem I supercomplex from Galdieria sulphuraria close to an ancestral red alga. *Science Advance* **11**, 2375-2548, doi:10.1126/sciadv.adv7488 (2025).

5 Shao, R. *et al.* Architecture of photosystem I–light-harvesting complex from the eukaryotic filamentous yellow-green alga Tribonema minus. *Journal of Integrative Plant Biology*, 3014-3031, doi:10.1111/jipb.70010 (2025).

6 Nagao, R. *et al.* Structural basis for assembly and function of a diatom photosystem I-light-harvesting supercomplex. *Nature Communications* **11**, doi:10.1038/s41467-020-16324-3 (2020).

7 Xu, C. *et al.* Structural basis for energy transfer in a huge diatom PSI-FCPI supercomplex. *Nature Communications* **11**, doi:10.1038/s41467-020-18867-x (2020).

8 Feng, Y. *et al.* Structures of PSI–FCPI from Thalassiosira pseudonana grown under high light provide evidence for convergent evolution and light-adaptive strategies in diatom FCPIs. *Journal of Integrative Plant Biology* **67**, 949-966, doi:10.1111/jipb.13816 (2024).

9 Zhang, S. *et al.* Growth phase-dependent reorganization of cryptophyte photosystem I antennae. *Communications Biology* **7**, doi:10.1038/s42003-024-06268-5 (2024).

10 Zhao, L.-S. *et al.* Structural basis and evolution of the photosystem I–light-harvesting supercomplex of cryptophyte algae. *The Plant Cell* **35**, 2449-2463, doi:10.1093/plcell/koad087 (2023).

11 Fei-Yu He, L.-S. Z., Xin-Xiao Qu, Kang Li, Jian-Ping Guo, Fang Zhao, Ning Wang, Bing-Yue Qin, Xiu-Lan Chen, Jun Gao, Lu-Ning Liu, and YuZhong Zhang. Structural insights into the assembly and energy transfer of haptophyte photosystem I-light-harvesting supercomplex. *Proceedings of the National Academy of Sciences* **121**, doi:10.1073/pnas (2024).

12 Shen, L. *et al.* Structure and function of a huge photosystem I–fucoxanthin chlorophyll supercomplex from a coccolithophore. *Science* **389**, doi:10.1126/science.adv2132 (2025).

13 Zhao, L.-S. *et al.* Architecture of symbiotic dinoflagellate photosystem I–light-harvesting supercomplex in Symbiodinium. *Nature Communications* **15**, doi:10.1038/s41467-024-46791-x (2024).

14 Xiaoyi Li, Z. L., Fangfang Wang, Songhao Zhao, Caizhe Xu, Zhiyuan Mao, Jialin Duan, Yue Feng, Yang Yang, Lili Shen,, Guanglei Wang, Y. Y., Long-Jiang, Yu, M. S., Guangye Han, Xuchu Wang, Tingyun Kuang, Jian-Ren, Shen & Wang, a. W. Structures and organizations of PSI–AcpPCI supercomplexes from red tidal and coral symbiotic photosynthetic dinoflagellates. *Proceedings of the National Academy of Sciences* **121**, doi:10.1073/pnas (2024).

15 Pan, X. *et al.* Structural basis of LhcbM5-mediated state transitions in green algae. *Nature Plants* **7**, 1119-1131, doi:10.1038/s41477-021-00960-8 (2021).

16 Su, X. *et al.* Antenna arrangement and energy transfer pathways of a green algal photosystem-I–LHCI supercomplex. *Nature Plants* **5**, 273-281, doi:10.1038/s41477-019-0380-5 (2019).

17 Naschberger, A. *et al.* Algal photosystem I dimer and high-resolution model of PSI-plastocyanin complex. *Nature Plants* **8**, 1191-1201, doi:10.1038/s41477-022-01253-4 (2022).

18 Qin, X. *et al.* Structure of a green algal photosystem I in complex with a large number of light-harvesting complex I subunits. *Nature Plants* **5**, 263-272, doi:10.1038/s41477-019-0379-y (2019).

19 Caspy, I. *et al.* Structure and energy transfer pathways of the Dunaliella Salina photosystem I supercomplex. *Biochimica et Biophysica Acta Bioenergetics* **1861**, 148253, doi:10.1016/j.bbabio.2020.148253 (2020).

20 Ishii, A. *et al.* The photosystem I supercomplex from a primordial green alga Ostreococcus tauri harbors three light-harvesting complex trimers. *Elife* **12**, doi:10.7554/eLife.84488 (2023).

21 Sun, H., Shang, H., Pan, X. & Li, M. Structural insights into the assembly and energy transfer of the Lhcb9-dependent photosystem I from moss Physcomitrium patens. *Nature Plants* **9**, 1347-1358, doi:10.1038/s41477-023-01463-4 (2023).

22 Gorski, C. *et al.* The structure of the Physcomitrium patens photosystem I reveals a unique Lhca2 paralogue replacing Lhca4. *Nature Plants* **8**, 307-316, doi:10.1038/s41477-022-01099-w (2022).

23 Yan, Q. *et al.* Antenna arrangement and energy-transfer pathways of PSI-LHCI from the moss Physcomitrella patens. *Cell Discovery* **7**, 10, doi:10.1038/s41421-021-00242-9 (2021).

24 Zhang, S. *et al.* Structural insights into a unique PSI-LHCI-LHCII-Lhcb9 supercomplex from moss Physcomitrium patens. *Nature Plants* **9**, 832-846, doi:10.1038/s41477-023-01401-4 (2023).

25 Xiaowei Pan, J. M., Xiaodong Su, Peng Cao, Wenrui Chang, Zhenfeng Liu, Xinzheng Zhang, Mei Li. Structure of the maize photosystem I supercomplex with light-harvesting complexes I and II. *Science* **360**, 1109-1113, doi:10.1126/science.aat1156 (2018).

26 Xiaochun Qin, M. S., Tingyun Kuang, Jian-Ren Shen. Structural basis for energy transfer pathways in the plant PSI-LHCI supercomplex. *Science* **348**, 989-995, doi:10.1126/science.aab0214 (2015).